KURENAI
Kyoto University Research Information Repository

KYOTO UNIVERSITY

Title	Observation of high Rydberg states of one-dimensional excitons in GaAs quantum wires by magnetophotoluminescence excitation spectroscopy
Author(s)	Okano, Makoto; Kanemitsu, Yoshihiko; Chen, Shaoqiang; Mochizuki, Toshimitsu; Yoshita, Masahiro; Akiyama, Hidefumi; Pfeiffer, Loren N.; West, Ken W.
Citation	Physical Review B (2012), 86(8)
Issue Date	2012-08-16
URL	http://hdl.handle.net/2433/159454
Right	©2012 American Physical Society
Type	Journal Article
Textversion	publisher

Observation of high Rydberg states of one-dimensional excitons in GaAs quantum wires by magnetophotoluminescence excitation spectroscopy

Makoto Okano,[1,*] Yoshihiko Kanemitsu,[1] Shaoqiang Chen,[2] Toshimitsu Mochizuki,[2] Masahiro Yoshita,[2]
Hidefumi Akiyama,[2] Loren N. Pfeiffer,[3] and Ken W. West[3]

[1]*Institute for Chemical Research, Kyoto University, Uji, Kyoto 611-0011, Japan*
[2]*Institute for Solid State Physics, University of Tokyo, Kashiwa, Chiba 277-8581, Japan*
[3]*Department of Electrical Engineering, Princeton University, Princeton, New Jersey 08540, USA*
(Received 5 March 2012; revised manuscript received 29 July 2012; published 16 August 2012)

We have studied the higher Rydberg states of the ground exciton in T-shaped GaAs quantum wires with low-temperature photoluminescence excitation spectroscopy under magnetic fields. The peak of the second even-parity Rydberg state appears and grows in intensity at the onset of the one-dimensional (1D) continuum edge under strong magnetic fields. In stark contrast to the ground exciton, it shows significantly low zero-field oscillator strength and a large diamagnetic shift. These characteristic features are attributed to the extremely weakly bound wave function of the second Rydberg state, reflecting the inherent and novel character of 1D excitons that was predicted theoretically.

I. INTRODUCTION

The optical properties of one-dimensional (1D) quantum structures have attracted considerable interest from the viewpoint of fundamental physics and for high-performance device applications.[1] Because of the spatial carrier confinement in 1D structures, the strong Coulomb interaction between conduction-band electrons and valence-band holes causes stable excitons to be formed.[2] Optical transitions are concentrated at the lowest exciton, and the band-to-band absorption is either extremely weak or not observed in the linear absorption spectra.[3,4] Because the stable exciton plays an important role in determining optical properties, the excitonic structures in various 1D nanomaterials, such as GaAs quantum wires,[5,6] carbon nanotubes,[7–9] and Si polymers,[10] have been extensively studied. Recently, remarkable progress has been achieved in high-quality 1D quantum-structure fabrication methods,[11–14] indicating that a clear and direct observation of excited-exciton states in 1D systems is possible. In particular, 1D GaAs wires fabricated by molecular-beam epitaxy (MBE) offer some advantages for use in optoelectronic devices because of their embedded structures.[15]

Numerous studies have been conducted on the excited-exciton states in semiconductor quantum wires.[6,16–24] The observed excited-exciton states consist of higher electron and higher hole subbands or different electron and hole subbands. The higher Rydberg states of the ground exciton, consisting of the first electron and the first hole subbands, are indistinguishable from the band edge and other possible excited-subband transitions because of their small binding energies and broadening. Thus, the higher Rydberg state excitons in GaAs quantum wires with a quantum number $n > 1$ have never been verified to date. However, the experimental verification of the higher Rydberg state excitons is very important.

Theoretically, peculiar characteristics of 1D exciton structures are predicted to manifest themselves in the form of the stark contrast between the properties of the lowest and higher Rydberg states of 1D excitons.[3,4] Both the binding energy and the oscillator strength of the lowest Rydberg states are significantly increased as 1D confinement becomes stronger, whereas those of the higher Rydberg states are expected to typically decrease[3] and may show anomalous dependence of 1D excitons on the effective 1D Coulomb interaction strength.[4] Despite their significance in 1D exciton physics, the detailed properties of higher Rydberg state excitons have not been determined experimentally thus far for any of the 1D nanostructures, including carbon nanotubes. In order to gain an insight into the nature of 1D excitons, a direct comparison between the lowest and higher Rydberg states of 1D excitons is needed. Moreover, a better understanding of high-energy exciton states would provide a detailed insight into nonlinear optical processes and multiexciton processes such as quantized Auger recombination[25–27] and multiple exciton generation.[28,29]

In this article, we report the first direct observation of the higher Rydberg states of 1D excitons using multidirectional magneto-photoluminescence excitation (PLE) spectroscopy at low temperatures, which provides systematic and quantitative access to higher Rydberg state excitons in 1D systems. PLE spectra of T wires show anisotropic magnetic-field dependence, providing direct experimental evidence of T-shaped quantum confinements. These magnetic effects intensify the peaks in the PLE spectra of T-wire excitons and reveal the internal structure of 1D excitons. The second even-parity Rydberg state appeared near the 1D continuum edge, and its intensity increased with the magnetic field. We observed low oscillator strength and a large diamagnetic blueshift for the second Rydberg state, in contrast to those of the exciton ground state. These observations reveal an intriguing contrast between the strongly and weakly bound wave functions of the ground and the higher Rydberg states of 1D excitons. This contrast can be attributed to the inherent characteristics of 1D excitons.

II. EXPERIMENT

Highly uniform 100-period T wires were fabricated by MBE with cleaved-edge-overgrowth and growth-interrupt annealing techniques.[11,12] Figure 1(a) shows the cross-sectional scanning transmission electron microscopy (TEM) image of a 100 T-wire laser structure. The 100 T wires were formed at
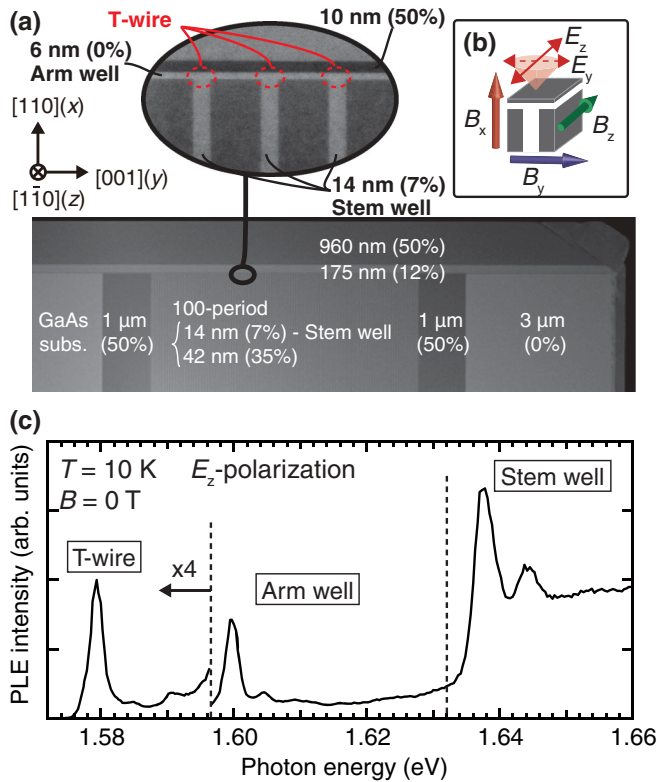
FIG. 1. (Color online) (a) Cross-sectional scanning TEM images of 100-period *T*-wire lasers. Percentages represent the Al content *x* of $Al_xGa_{1-x}As$. *T* wires are formed at the *T* intersections of the 100-period stem wells and the arm well as shown in the enlarged view (upper portion). (b) Schematic of the PLE experiment configuration. (c) Typical PLE spectrum of 100 *T* wires at 0 T under E_z polarization.

100 *T*-shaped intersections of 100 period (001) $Al_{0.07}Ga_{0.93}As$ multiple quantum wells (stem wells) and a (110) GaAs quantum well (arm well). The thicknesses of the stem and arm wells were 14 and 6 nm, respectively. In the first MBE growth on a (001) undoped GaAs substrate, we successively formed a 0.5-μm GaAs buffer layer, a 1-μm $Al_{0.5}Ga_{0.5}As$ side-cladding layer, a 100-period $Al_{0.07}Ga_{0.93}As/Al_{0.35}Ga_{0.65}As$ multiple-quantum-well structure with barrier and quantum well thicknesses of 42 and 14 nm, respectively, a 1.0-μm $Al_{0.5}Ga_{0.5}As$ side-cladding layer, and a cap layer of 3-μm GaAs. On an *in situ* cleaved (110) surface of the wafer, we overgrew a 6-nm GaAs quantum well (undoped) followed by a 10-nm $Al_{0.5}Ga_{0.5}As$ barrier, a 175-nm $Al_{0.12}Ga_{0.88}As$ optical arm, which acts as an optical core layer, a 0.96-μm $Al_{0.5}Ga_{0.5}As$ upper cladding layer, and a 10-nm GaAs cap layer; all layers were undoped.

In the PLE measurements, the excitation light from a continuous-wave titanium-sapphire laser was focused to a spot a few micrometers in diameter on the (110) surface of the sample by using a 0.5 numerical aperture objective lens. The sample was mounted onto the cold finger in a He-flow-type cryostat. The polarization of laser light was set perpendicular (E_y) or parallel (E_z) to the *T* wires for revealing the selection rule of the optical transitions. Photoluminescence (PL) was collected via the same objective lens. A polarizer positioned in a direction normal to the incident polarization reduced

scattering from the excitation laser. Polarization-selective PL detections do not alter measured PLE spectral shapes, because PL occurs only from the ground-state excitons in the *T* wires with a fixed polarization anistropy. To eliminate stray light from intense laser backscattering, we tilted the sample approximately 20° off normal incidence to the backscattering geometry. The notations for the excitation-light polarizations and applied magnetic-field conditions in this work are shown in Fig. 1(b).

III. RESULTS AND DISCUSSION

Figure 1(c) shows a typical PLE spectrum of *T* wires at 10 K in the absence of a magnetic field. The lowest PLE peak at 1.579 eV is assigned to the first Rydberg state of the ground exciton in the *T* wires, consisting of the first electron and first hole subbands (denoted as *E1H1n1*). This spectrum has four other PLE peaks at 1.600, 1.604, 1.637, and 1.644 eV. These are also assigned to the heavy-hole excitons in the arm well on the core layer, in the arm well on the cladding layer, in the stem wells, and the light-hole exciton in the stem wells, respectively.[22,30] The full width at half maximum of the *E1H1n1* exciton PLE peak is about 2 meV, indicating the high uniformity of the 100 *T* wires. The continuous PLE band above 1.590 eV comes from 1D-exciton transitions due to higher hole subbands, higher Rydberg states, and ionized continuum states. These states cannot be distinguished from each other in the absence of a magnetic field.

Figure 2 shows the magnetic-field dependence of the PLE spectra of the *T* wires at 10 K. These spectra were normalized at the *E1H1n1* exciton peak. Magnetic fields were applied along the *x* (B_x field, red curves) or *y* axes (B_y field, blue
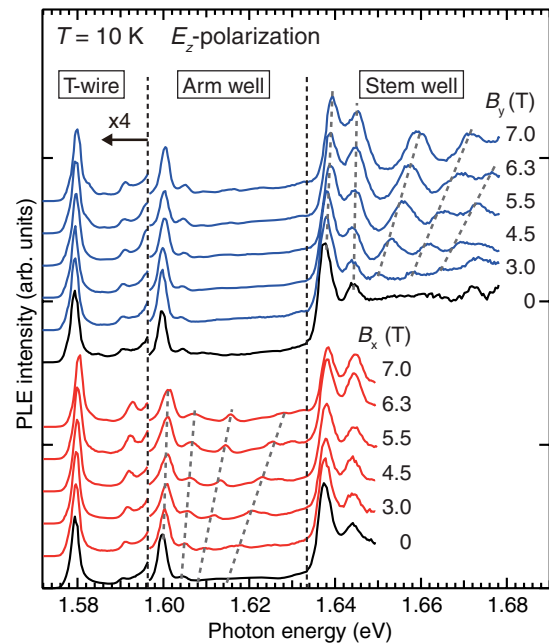

FIG. 2. (Color online) Magnetic-field dependence of PLE spectra of 100 *T* wires at 10 K under E_z polarization. The black curves represent the PLE spectra at 0 T. The red and blue curves correspond to the B_x and B_y fields, respectively. These spectra are normalized to the lowest exciton peak.
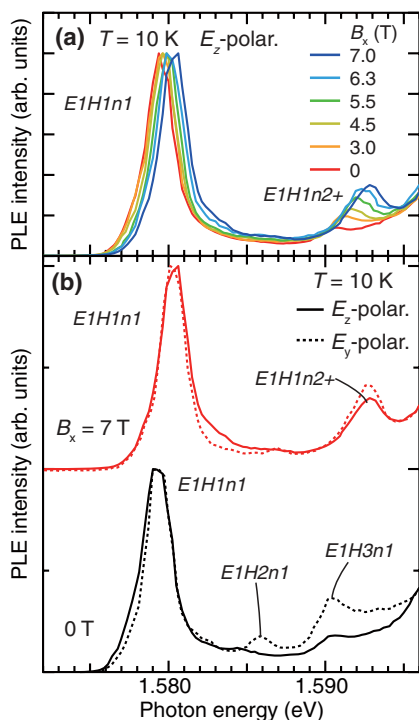
FIG. 3. (Color online) (a) B_x dependence of PLE spectra of excitonic structures in T wires at 10 K. Excitation light is polarized to the E_z direction. (b) Polarization dependence of the excitonic structures in T wires at 0 (black curves) and 7 T (red curves). The E_z and E_y polarizations are represented by the solid and broken curves, respectively. All spectra in these figures are normalized to the lowest exciton peak.

curves), and the excitation-light polarization was parallel to the z axis along the T wires (E_z polarization). The PLE structures of the stem wells (arm well) appear to be insensitive to the B_x (B_y) field, but the peaks appear due to the Landau levels and their energies blue-shift with an increase in the B_y (B_x) field. No significant magnetic-field dependence of the $E1H1n1$ exciton peak was observed, demonstrating that our magneto-PLE spectra provide direct experimental evidence of 1D quantum confinements, in contrast to magneto-PL spectra.[31] In the PLE spectra, the unique Landau fan diagrams, dependent on the magnetic-field orientations, provide the direct assignment of the peaks to the two quantum wells and T wire with different quantum-confinement configurations.

Figures 3(a) and 3(b) show enlarged views of the magnetic-field dependence and the polarization dependence of the 1D exciton in the PLE spectra. The spectra were normalized at the $E1H1n1$ exciton peak around 1.580 eV. We can clearly observe that the new peak appears at the continuous edge in Fig. 3(a). The new and the $E1H1n1$ exciton peaks shift to higher energy with increasing magnetic field. The solid and broken curves correspond to the PLE spectra for E_z and E_y polarizations in Fig. 3(b). At 0 T, the PLE spectra (black curves) show strong polarization dependence in the energy region between 1.585 and 1.595 eV, which includes the small peaks at 1.586 and 1.590 eV. Note that for $B_x = 7$ T (red curves), the polarization dependence is almost diminished.

Because it is well known that the polarization dependence of the absorption and PLE spectra in GaAs quantum wires

originates from the anisotropy of hole states,[19,20,22,32,33] the observed polarization-dependent peaks at 1.586 and 1.590 eV are due to the higher hole subbands. By a previous detailed study in comparison with theoretical calculations,[22] the peaks at 1.586 and 1.590 eV at 0 T are assigned to the 1D exciton states formed with the first-subband electron and the second- or third-subband hole (denoted as $E1H2n1$ and $E1H3n1$), respectively. Indeed, these contributions are stronger for E_y polarizations, which is a polarization for the weakest $E1H1$ transition. In contrast, the quenched polarization dependence at $B_x = 7$ T indicates that the transitions due to the higher hole subbands, such as $E1H2n1$ and $E1H3n1$, are quenched. This suggests that the rigid optical transition selection rules are realized under strong magnetic fields, therefore, all absorption structures at 7 T are not due to the higher hole subbands but due to the $E1H1$ transition, with $E1H1n1$ being the most common. Thus, the polarization-independent absorption peak found at 1.593 eV under $B_x = 7$ T is assigned to the next optically allowed $n = 2$ even-parity Rydberg state of the $E1H1$ excitons (denoted as $E1H1n2+$) because the $n = 2$ odd-parity Rydberg state of the $E1H1$ excitons is optically forbidden.[22] The energy position of second even-parity Rydberg state is in good agreement with theoretical calculation.[22] The second Rydberg state has never been observed experimentally thus far.

Figure 4 shows the PLE intensity ratios of the $E1H1n2+$ peak (filled circles) in E_z polarization and the $E1H2n1$ peak (open circles) in E_y polarization to the $E1H1n1$ peak as a function of B_x^2. As the applied field increases, the ratio of $E1H2n1$ to $E1H1n1$ excitons decreases. This indicates that the optical transition selection rules become stricter. In contrast, the ratio of $E1H1n2+$ to $E1H1n1$ excitons becomes larger with increasing magnetic field. By a simple model calculation for 1D systems,[34] the magnetic-field-dependent change in the oscillator strength ratio of the second to the first Rydberg state is due to the change in the ratio of the cyclotron energy to the subband energy splitting or the lateral confinement energy. For our study samples, the lateral confinement energy corresponds
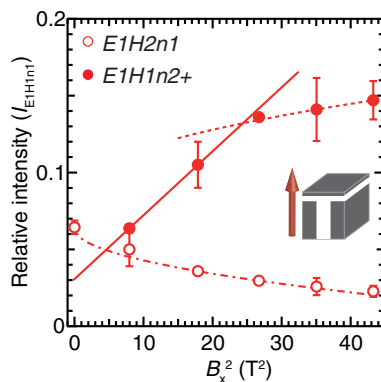

FIG. 4. (Color online) Intensity ratios of the $E1H2n1$ (open circles) and $E1H1n2+$ (filled circles) excitons to the $E1H1n1$ exciton as a function of the square of the magnetic field B_x. The polarizations of the laser light are E_z for the $E1H1n2+$ exciton and E_y for the $E1H2n1$ exciton, respectively. The solid and broken lines represent the linear and the square root functions. The dash-dotted line is solely for reference.

to the energy difference between the ground exciton in the *T* wire and that in the arm well. When the cyclotron energy is far smaller than the zero-field subband energy splitting, the oscillator strength ratio shows quadratic dependence with *B*. However, when the cyclotron energy is far larger than the zero-field subband energy splitting, the oscillator strength ratio shows linear dependence with *B*. A crossover between the quadratic and linear regimes in the dependence on *B* field should occur when these energies are comparable.

The experimental result can be fitted by a linear function (dotted line) at $B_x^2 < 30$ and a square-root function (solid line) at $B_x^2 > 30$, as expected by the model calculation.[34] The results suggest that the cyclotron energy becomes comparable to the subband energy splitting at 5.5 T. The cyclotron energy is estimated to be 12 meV at 5.5 T using the following parameters: the reduced mass of electrons and holes $\mu = 0.042\, m_0$, which is obtained by $m_e = 0.067 m_0$ and $m_h = 0.11 m_0$.[35] This energy is almost half the lateral confinement energy of 21 meV. Therefore, the observed crossover in the magnetic-field dependence appears to be reasonable.[34]

By interpolating the linear function to 0 T, the oscillator-strength ratio of the *E1H1n2+* to *E1H1n1* excitons at 0 T is estimated to be about 3×10^{-2}. This ratio is notably smaller than the ratio 7×10^{-2} of the second (2s) to the first (1s) allowed Rydberg states in a two-dimensional (2D) quantum well with 6-nm thickness.[36] This comparison between the optically-allowed second-lowest Rydberg states of 1D and 2D excitons demonstrates the first quantitative observation of small oscillator strength of the second Rydberg state of 1D excitons and reflects the nature of the 1D exciton in which the oscillator strength is concentrated in the lowest exciton state.[3,4] It should be noted that the difference in oscillator strengths among different Rydberg states stems from the difference in the value of the squared wave function for electron-hole relative motion r_{e-h} at the origin $r_{e-h} = 0$. Therefore, the present small oscillator-strength ratio can be interpreted as demonstrating a remarkable contrast between the strongly and weakly bound wave functions of the ground and the high Rydberg states of 1D excitons.

The peak energies of the *E1H1n1* and *E1H1n2+* excitons are plotted as a function of B^2 in Fig. 5(a). The red, blue, and green circles are the data under B_x, B_y, and B_z fields, respectively. The data for the *E1H1n2+* exciton at 0 T are excluded from the graph. It is observed that the energy shifts of the *E1H1n1* and *E1H1n2+* excitons are proportional to B^2 in all magnetic-field directions. These excitons show the anisotropic magnetic-field dependence due to *T*-shaped quantum confinement. By interpolating the energies of the *E1H1n1* and *E1H1n2+* excitons to 0 T, the energy difference between the two states is evaluated as 11.4 meV. This result is close to the calculated binding energy of the ground exciton, 13.5 ± 0.5 meV,[37] indicating the weak binding of the *E1H1n2+* exciton.

When the cyclotron radius is larger than the exciton Bohr radius, the magnetic-field dependence of the energy shift of excitons ΔE, the so-called diamagnetic shift, is expressed as $\Delta E = e^2 \langle r^2 \rangle / 8\mu B^2 \equiv \beta B^2$.[38] Here *e* is the elementary charge, $\langle r^2 \rangle$ is the effective area of the excitons in the plane perpendicular to the magnetic field at 0 T, and β is the diamagnetic coefficient, which is a positive value. Figure 5(b)
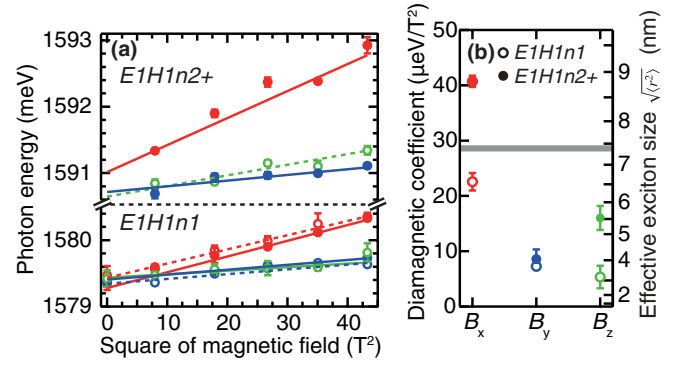

FIG. 5. (Color online) The square of the applied magnetic-field dependencies of peak positions of *E1H1n1* and *E1H1n2+* excitons. The filled (open) circles and solid (broken) lines correspond to E_z (E_y) polarization. (b) The diamagnetic coefficient of *E1H1n1* (open circles) and *E1H1n2+* (filled circles) excitons under B_x, B_y, and B_z fields. The right ordinate shows the effective exciton size. Red, blue, and green circles and lines correspond to the influence of B_x, B_y, and B_z fields, respectively.

plots the coefficient β, derived from Fig. 5(a), of each exciton peak as a function of magnetic-field direction. The right ordinate shows the effective exciton size, $\sqrt{\langle r^2 \rangle}$ derived from the diamagnetic coefficients. The coefficient of the *E1H1n1* exciton is 22.2 μeV/T^2 for the B_x field, which is smaller than the 2D quantum limit (28.3 μeV/T^2), indicated by the gray hatched line. The coefficient of the *E1H1n2+* exciton is 41 μeV/T^2 for the B_x field, which is larger than the 2D quantum limit. The coefficient of the *E1H1n2+* exciton is larger than that of the *E1H1n1* exciton in all magnetic-field directions. In particular, the coefficients of the *E1H1n2+* exciton are twice as large as those of the *E1H1n1* exciton in B_x and B_z fields. In addition to the polarization dependence of PLE spectra, these features strongly support the assignment that the *E1H1n2+* exciton is a higher Rydberg state of the *E1H1n1* exciton. Note, $\sqrt{\langle r^2 \rangle}$ is determined by lateral confinement due to the heterostructure and the exciton's electron-hole Coulomb interaction. The observed difference in $\sqrt{\langle r^2 \rangle}$ between the *E1H1n1* and *E1H1n2+* excitons is due to the difference in the exciton confinement. This also provides evidence of the contrast in binding between the ground and the higher Rydberg states of 1D excitons.

IV. CONCLUSION

In summary, we determined the oscillator strength and diamagnetic shift of 1D excitons in *T*-shaped GaAs quantum wires. The oscillator strength of the *E1H1n2+* exciton is 3×10^{-2} lower than that of the *E1H1n1* exciton. The diamagnetic coefficient of the *E1H1n2+* exciton is notably larger than that of the *E1H1n1* exciton. These results demonstrate the pronounced contrast between the ground and the higher Rydberg states as a unique and inherent characteristic of 1D excitons. Therein, only the ground exciton is strongly bound, while the higher Rydberg excitons are weakly bound.

*okano.makoto.4a@kyoto-u.ac.jp

[1] H. Haug and S. W. Koch, *Quantum Theory of the Optical and Electronic Properties of Semiconductors*, 5th ed. (World Scientific, Singapore, 2009).

[2] R. Loudon, Am. J. Phys. **27**, 649 (1959).

[3] T. Ogawa and T. Takagahara, Phys. Rev. B **44**, 8138 (1991).

[4] T. Ando, J. Phys. Soc. Jpn. **74**, 777 (2005), and references therein.

[5] E. Kapon, D. M. Hwang, and R. Bhat, Phys. Rev. Lett. **63**, 430 (1989).

[6] M. Yoshita, S. M. Liu, M. Okano, Y. Hayamizu, H. Akiyama, L. N. Pfeiffer, and K. W. West, J. Phys.: Condens. Matter **19**, 295217 (2007), and references therein.

[7] F. Wang, G. Dukovic, L. E. Brus, and T. F. Heinz, Science **308**, 838 (2005); J. Maultzsch, R. Pomraenke, S. Reich, E. Chang, D. Prezzi, A. Ruini, E. Molinari, M. S. Strano, C. Thomsen, and C. Lienau, Phys. Rev. B **72**, 241402 (2005).

[8] J. Lefebvre and P. Finnie, Nano Lett. **8**, 1890 (2008).

[9] Y. Kanemitsu, Phys. Chem. Chem. Phys. **13**, 14879 (2011), and references therein.

[10] T. Hasegawa, Y. Iwasa, H. Sunamura, T. Koda, Y. Tokura, H. Tachibana, M. Matsumoto, and S. Abe, Phys. Rev. Lett. **69**, 668 (1992).

[11] L. N. Pfeiffer, K. W. West, H. L. Stormer, J. P. Eisenstein, K. W. Baldwin, D. Gershoni, and J. Specter, Appl. Phys. Lett. **56**, 1697 (1990).

[12] M. Yoshita, H. Akiyama, L. N. Pfeiffer, and K. W. West, Appl. Phys. Lett. **81**, 49 (2002).

[13] M. J. O'Connell, S. M. Bachilo, C. B. Huffman, V. C. Moore, M. S. Strano, E. H. Haroz, K. L. Rialon, P. J. Boul, W. H. Noon, C. Kittrell, J. Ma, R. H. Hauge, R. B. Weisman, and R. E. Smalley, Science **297**, 593 (2002).

[14] X. Tu, S. Manohar, A. Jagota, and M. Zheng, Nature **460**, 250 (2009).

[15] For example, L. A. Coldren, S. W. Corzine, and M. L. Mashanovitch, *Diode Lasers and Photonic Integrated Circuits*, 2nd ed. (Wiley, New York, 2012).

[16] R. Rinaldi, R. Cingolani, M. Lepore, M. Ferrara, I. M. Catalano, F. Rossi, L. Rota, E. Molinari, P. Lugli, U. Marti, D. Martin, F. Morier-Gemoud, P. Ruterana, and F. K. Reinhart, Phys. Rev. Lett. **73**, 2899 (1994).

[17] H. Weman, M. Potemski, M. E. Lazzouni, M. S. Miller, and J. L. Merz, Phys. Rev. B **53**, 6959 (1996).

[18] W. R. Tribe, M. J. Steer, D. J. Mowbray, M. S. Skolnick, A. N. Forshaw, J. S. Roberts, G. Hill, M. A. Pate, C. R. Whitehouse, and G. M. Williams, App. Phys. Lett. **70**, 993 (1997).

[19] T. Sogawa, H. Ando, S. Ando, and H. Kanbe, Phys. Rev. B **56**, 1958 (1997).

[20] F. Vouilloz, D. Y. Oberli, M.-A. Dupertuis, A. Gustafsson, F. Reinhardt, and E. Kapon, Phys. Rev. Lett. **78**, 1580 (1997).

[21] M. Bayer, Ch. Schlier, Ch. Gréus, A. Forchel, S. Benner, and H. Haug, Phys. Rev. B **55**, 13180 (1997).

[22] H. Itoh, Y. Hayamizu, M. Yoshita, H. Akiyama, L. N. Pfeiffer, K. W. West, M. H. Szymanska, and P. B. Littlewood, App. Phys. Lett. **83**, 2043 (2003).

[23] N. I. Cade, R. Roshan, M. Hauert, A. C. Maciel, J. F. Ryan, A. Schwarz, Th. Schäpers, and H. Lüth, Phys. Rev. B **70**, 195308 (2004).

[24] S. Palmgren, H. Weman, A. Schoenberg, K. F. Karlsson, M.-A. Dupertuis, K. Leifer, A. Rudra, and E. Kapon, Appl. Phys. Lett. **89**, 191111 (2006).

[25] F. Wang, G. Dukovic, L. E. Brus, and T. F. Heinz, Phys. Rev. Lett. **92**, 177401 (2004).

[26] V. I. Klimov, A. A. Mikhailovsky, D. W. McBranch, C. A. Leatherdale, and M. G. Bawendi, Science **287**, 1011 (2000).

[27] Y.-Z. Ma, L. Valkunas, S. L. Dexheimer, S. M. Bachilo, and G. R. Fleming, Phys. Rev. Lett. **94**, 157402 (2005): L. Huang and T. D. Krauss, Phys. Rev. Lett. **96**, 057407 (2006).

[28] A. Ueda, K. Matsuda, T. Tayagaki, and Y. Kanemitsu, App. Phys. Lett. **92**, 233105 (2008); S. Wang, M. Khafizov, X. Tu, M. Zheng, and T. D. Krauss, Nano Lett. **10**, 2381 (2010).

[29] N. M. Gabor, Z. Zhong, K. Bosnick, J. Park, and P. L. McEuen, Science **325**, 1367 (2009).

[30] H. Akiyama, M. Yoshita, L. N. Pfeiffer, K. W. West, and A. Pinczuk, App. Phys. Lett. **82**, 379 (2003).

[31] T. Someya, H. Akiyama, and H. Sakaki, Phys. Rev. Lett. **74**, 3664 (1995); Solid State Commun. **108**, 923 (1998).

[32] M. A. Dupertuis, E. Martinet, D. Y. Oberli, and E. Kapon, Europhys. Lett. **52**, 420 (2000).

[33] S. Watanabe, M. Yoshita, S. Koshiba, and H. Akiyama, Jpn. J. Appl. Phys. **41**, 5924 (2002).

[34] S. Benner and H. Haug, Phys. Rev. B **47**, 15750 (1993).

[35] M. Okano, P. Huai, M. Yoshita, S. Inada, H. Akiyama, K. Kamide, K. Asano, and T. Ogawa, J. Phys. Soc. Jpn. **80**, 114716 (2011).

[36] M. Gurioli, J. Martinez-Pastor, M. Colocci, A. Bosacchi, S. Franchi, and L. C. Andreani, Phys. Rev. B **47**, 15755 (1993).

[37] M. H. Szymanska, P. B. Littlewood, and R. J. Needs, Phys. Rev. B **63**, 205317 (2001).

[38] O. Akimoto and H. Hasegawa, J. Phys. Soc. Jpn. **22**, 181 (1967).